Temperature Dependence and Kinetic Isotope Effects for the OH + HBr Reaction and H/D Isotopic Variants at Low Temperatures (53−135 K) Measured Using a Pulsed Supersonic Laval Nozzle Flow Reactor

Christopher Mullen and Mark A. Smith*

Department of Chemistry, University of Arizona, 1306 E. University Dr., Tucson, Arizona 85721

Received: September 30, 2004; In Final Form: February 17, 2005

The reactions of OH + HBr and all isotopic variants have been measured in a pulsed supersonic Laval nozzle flow reactor between 53 and 135 K, using a pulsed DC discharge to create the radical species and laser induced fluorescence on the A $^2\Sigma \leftarrow$ X $^2\Pi$ ($v' = 1 \leftarrow v'' = 0$) transition. All reactions are found to possess an inverse temperature dependence, in accord with previous work, and are fit to the form $k = A(T/298)^{-n}$, with k_1 (OH + HBr) = $(10.84 \pm 0.31) \times 10^{-12}(T/298)^{(-0.67\pm0.02)}$ cm^3/s, k_2 (OD + HBr) = $(6.43 \pm 2.60) \times 10^{-12}(T/298)^{(-1.19\pm0.26)}$ cm^3/s, k_3 (OH + DBr) = $(5.89 \pm 1.93) \times 10^{-12}(T/298)^{(-0.76\pm0.22)}$ cm^3/s, and k_4 (OD + DBr) = $(4.71 \pm 1.56) \times 10^{-12}(T/298)^{(-1.09\pm0.21)}$ cm^3/s. A global fit of k vs T over the temperature range 23−360 K, including the new OH + HBr data, yields $k(T) = (1.06 \pm 0.02) \times 10^{-11}(T/298)^{(-0.90\pm0.11)}$ cm^3/s, and $(0.96 \pm 0.02) \times 10^{-11}(T/298)^{(-0.90\pm0.03)} \exp^{((-2.88\pm1.82\ \mathrm{K})/T)}$ cm^3/s, in accord with previous fits. In addition, the primary and secondary kinetic isotope effects are found to be independent of temperature within experimental error over the range investigated and take on the value of $(k_H/k_D)_{AVG} = 1.64$ for the primary effect and $(k_H/k_D)_{AVG} = 0.87$ for the secondary effect. These results are discussed within the context of current experimental and theoretical work.

Introduction

The reaction of OH + HBr → H_2O + Br and the isotopic variants has been studied both experimentally and theoretically in the past by a number of different research groups.

$$\mathrm{OH + HBr \xrightarrow{k_1} H_2O + Br} \quad \text{(R1)}$$

$$\mathrm{OD + HBr \xrightarrow{k_2} HOD + Br} \quad \text{(R2)}$$

$$\mathrm{OH + DBr \xrightarrow{k_3} DOH + Br} \quad \text{(R3)}$$

$$\mathrm{OD + DBr \xrightarrow{k_4} D_2O + Br} \quad \text{(R4)}$$

Motivation for doing so has been two-fold. First, the reaction affects the Br partitioning in the middle to lower stratosphere of earth's atmosphere. Bromine has been implicated as a species known to react with ozone creating BrO and O_2, and therefore, a rigorous understating of the reaction network surrounding Br creation and destruction has been sought. In addition, the kinetics of the reaction of OH with HBr has been experimentally found to show a strong inverse temperature dependence below approximately 200 K, i.e., temperatures pertinent to the upper atmosphere and stratosphere. To date experiments on the OH + HBr system have been carried out in the temperature range from 23 to 416 K. Ravishankara et al. conducted the first temperature dependent study between 249 and 416 K using the technique of laser flash photolysis-resonance fluorescence and found the rate to be independent of temperature over the temperature window investigated, with a rate of $(1.19 \pm 0.14) \times 10^{-11}$ cm^3 s^{-1}.[1] This study was motivated by earlier measurements of k_1 at temperatures of 298 and 1925 K, by Takacs and Glass (298 K),[2] Smith and Zellner (298 K),[3] and Wilson et al. (1925 K),[4] who found the rate to be $(5.1 \pm 1.0) \times 10^{-12}$, $(4.5 \pm 1.0) \times 10^{-12}$, and 2.56×10^{-11} cm^3/s, respectively. Following these studies, additional measurements near room temperature were also made using a variety of techniques.[5−8] Sims et al. applied the pulsed laser photolysis-laser induced fluorescence technique to the ultra-cold gas-phase environment created in the Cinétique de Réaction en Ecoulement Supersonique Uniforme (CRESU) to study the reaction over the temperature range of 23−295 K and found the inverse temperature onset below 295 K.[9] Atkinson et al. also studied the temperature dependence of the kinetics of R1 using a pulsed supersonic Laval nozzle flow reactor over the temperature range 76−242 K and similarly found inverse temperature dependence.[10] The rate coefficient has been found to be pressure independent,[1,10,11] consistent with a bimolecular reaction mechanism.

More recently, a joint experimental effort was conducted between the Rowe and Smith groups in Rennes and Tucson, with the aim of reconciling the low-temperature data for the OH + HBr reaction,[12] and included new measurements between 48 and 224 K. The study produced temperature-dependent fits to the available data between 23 and 416 K of

$$k(T) = 1.11 \times 10^{-11}\left(\frac{T}{298}\right)^{-0.91} \text{ cm}^3\text{/s} \quad (1)$$

and

$$k(T) = 1.06 \times 10^{-11}\left(\frac{T}{298}\right)^{-0.91} \exp^{(-10.5K/T)} \text{ cm}^3\text{/s} \quad (2)$$

* To whom correspondence should be addressed. E-mail: msmith@u.arizona.edu.

10.1021/jp045540n CCC: $30.25
Published on Web 04/13/2005

which were deemed to accurately model the data below 350 K. These fits were also found to be in accord with the previous recommendations of the IUPAC Subcommittee on Gas Kinetic Data Evaluation for Atmopsheric Chemistry,[13] and that of JPL,[14] of

$$k(T) = 1.1 \times 10^{-11}\left(\frac{T}{298}\right)^{-0.8} \text{cm}^3/\text{s} \qquad (3)$$

and

$$k(T) = 1.1 \times 10^{-11} \exp\left[\frac{(0 \pm 250)K}{T}\right] \text{cm}^3/\text{s} \qquad (4)$$

respectively.

The dependence of reactivity on isotopomer for a chemical system is also of great importance. Deuterium enrichment found throughout the interstellar medium is well-known, and efforts to understand the origins of these effects have been conducted.[15,16] The enrichment arises due to differences in zero-point energies between the deuterated and nondeuterated species and is initiated via isotopic exchange chemistry, primarily in ion−molecule reactions involving H_3^+, CH_3^+, and $C_2H_2^+$ with HD.[17,18] Once the deuterated ions are formed, they participate in a variety of subsequent chemistries, including dissociative recombination, to pass on their deuterium content. In cold clouds, the exothermic D + OH → H + OD ($\Delta H_{rxn} = 810$ K) is speculated to influence the local D/H ratio,[19] and this chemistry is included in the modeling of such environments.[20] In addition, Lunine et al. point out that the D/H ratio in methane might provide a complimentary chemical test to the origin of Titan's atmosphere,[21] and therefore, knowledge of the subsequent chemistry for molecules of interstellar importance is crucial for a complete physiochemical description of the environment. Knowledge of the H/D atom abstraction reactions of OH/OD with HBr/DBr, while not of astrophysical relevance at the time, provides information on the dynamics of a neutral−radical abstraction reaction occurring over a potential energy surface without an apparent barrier. Efficient neutral−radical reactions are now well-known,[22] and the low-temperature measurement of their reaction rates will further help modeling efforts of low-temperature environments.

Two other studies have significantly contributed to the temperature dependent knowledge on not only the OH + HBr system but the isotopomers as well. The study of Bedjanian et al. used a mass spectrometric discharge-flow reactor to make measurements between 230 and 360 K, on the reactions R1 through R4.[23] Further, Jaramillo and Smith used the pulsed supersonic Laval nozzle flow reactor to study the kinetics of reactions R1 through R4.[24] These studies will be discussed in detail later, but for now it is prudent to say that knowledge of the kinetic isotope effect (KIE), whether they be primary or secondary in nature, helps to provide constraints to important regions of the reaction potential energy surface.

Theoretical efforts have also been conducted aimed at describing the potential energy surface and the inverse temperature dependence found from experiments. They are mentioned here and discussed further in context of the current results. Clary et al. performed quantum scattering calculations using the rotating bond approximation (RBA) on a LEPS potential energy surface and found good qualitative agreement between the temperature dependence predicted from the calculations and that experimentally observed, as well as qualitative agreement in magnitude with the rates.[25] Nizamov et al.[26] extended the understanding of this reaction with calculations using variational transition state theory on a modified LEPS potential energy surface, with the goal of understanding the nature of the kinetic isotope effects and the fraction of vibrational energy transferred to the departing H_2O, HDO, and D_2O molecules found from infrared chemiluminescence measurements by Butkovskaya and Setser.[27] In addition, a more recent direct ab initio dynamics calculation by Liu et al. has found a hydrogen bonded complex intermediate on the reactant side of the potential energy surface at energies lower than that of reactants, and the rate coefficients over a broad temperature range were calculated with improved canonical variational transition state theory with a small-curvature tunneling correction.[28]

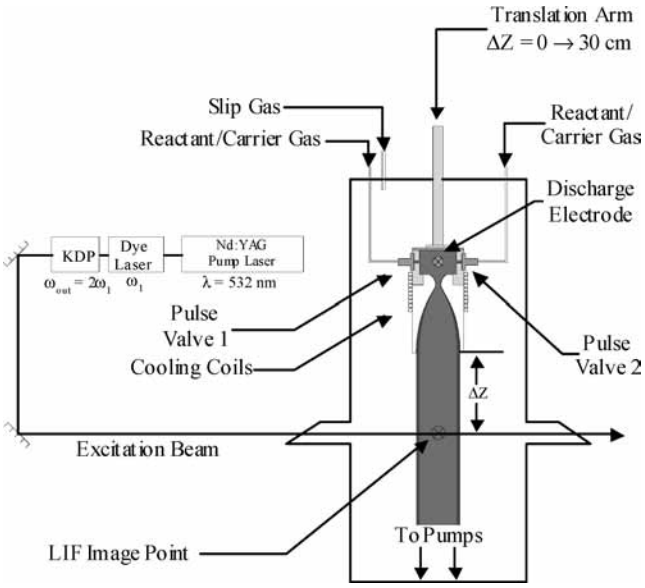

Figure 1. Schematic diagram of the pulsed supersonic Laval nozzle flow reactor.

The kinetic isotope effects measured by Bedjanian et al.[23] and Jaramillo and Smith[24] are extended in this study to lower temperatures between 53 and 135 K using the pulsed supersonic Laval nozzle flow reactor, in an effort to further understand the nature of the reaction PES, the temperature dependent KIEs observed in the two previous studies, and also to provide additional data necessary for the theoretical chemists to accurately describe the reaction mechanism, the entrance channel, and transition state dependence on the reactivity.

Experimental Section

A detailed description of our pulsed uniform supersonic expansion flow reactor is presented elsewhere, and thus, only a brief overview will be given here.[10,24] A schematic diagram of the instrument can be seen in Figure 1.

The kinetics of reactions R1 through R4 were studied by co-expanding known quantities of reagent and buffer gases through a supersonic pulsed Laval nozzle. An equilibrated flow ensues for a number of nozzle diameters past the nozzle exit (15−20 cm), at a well defined hydrodynamic velocity and density, allowing for enough time (approximately 300 μs) to perform kinetic measurements. The experiments were conducted such that the concentration of reagent [R], R = HBr or DBr, was much greater than that of the OH radical, ensuring that pseudo-first-order conditions were established. OH or OD radicals were created from water or deuterium oxide (Cambridge Isotopes Laboratories, Inc., 99.9%) precursors, using a pulsed DC discharge in the stagnation volume. The H_2O/D_2O was entrained

in the gas phase using a bubbler running with either N_2 (83 and 135 K) or Ar (53 K) depending on the buffer gas used for the experiment. In this manner, a mixture containing the partial pressure of H_2O divided by the total bubbler backing pressure (30 psig) could be delivered to the nozzle, in concentrations high enough to provide sufficient signal for the kinetic experiments. Using these numbers as a rough guide, the water concentration used was approximately 0.17%, 0.05%, and 0.03% of the total flow for the ArM32e16, N2M32e16, and N2M33e16 nozzle, respectively.

The time dependent OH/OD signal was monitored using laser induced fluorescence (LIF). Both OH and OD radicals were excited using the $A \leftarrow X$ ($^2\Sigma \leftarrow {}^2\Pi_{3/2}$, $v' = 1 \leftarrow v'' = 0$) transition, using a pulsed dye laser (Continuum model ND-60) pumped by a Nd:YAG operating on the second harmonic (Continuum model NY61). In both cases, kinetic experiments were conducted by monitoring the $S_{21}(1)$ line. For OH this occurs near 280.6 nm, whereas for OD it is at 286.9 nm. These wavelengths were created by doubling the output from the dye laser operating with Rhodamine 590 and a Rhodamine 590/610 mixture, respectively, in a KD*P crystal. The laser frequency was calibrated using the optogalvanic lines of Fe and Ne. The resulting (0,0) and (1,1) fluorescence was collected with a photomultiplier tube (Hamamatsu R3896) perpendicular to the flow, in conjunction with a 310 ± 10 nm band-pass filter and red pass filter (Schott WG29). The LIF signal was amplified and sent to either a boxcar averager (SRS 250) or oscilloscope (LeCroy 9400) and averaged for 200−500 shots. The gases used for these studies are as follows: N_2, US Airweld 99.99%; Ar, US Airweld; UHP, 99.999%; HBr, Matheson C. P. Grade 99.8%; DBr, Cambridge Isotope Laboratories, Inc. 99%. The HBr and DBr gases were each treated to three freeze−degas−thaw cycles with liquid nitrogen to remove the H_2 impurities. The rest were used without further modification.

Kinetic experiments are conducted after the flow exits the nozzle, by following the relative OH(OD) concentration as a function of distance in the flow. The reaction time is extracted from the distance between the probe laser and nozzle exit and is determined through knowledge of the flow velocity. This in turn is known from the flow Mach number obtained from impact and LIF measurements. The OH(OD) signal follows a single exponential decay, as evidenced by the linearity of the natural log of the normalized signal vs reaction time plot, Figure 2, indicating that pseudo-first order conditions have indeed be satisfied. The second order rate coefficient is extracted from a plot of the pseudo-first order decay constant versus the concentration of reactant under which it was obtained, Figure 3. The three nozzles used for this study have been previously characterized and as a result only their flow properties are shown here, Table 1.[29]

It is believed that under these experimental conditions the influence of secondary reactions on the extracted second order rate coefficient is minimized. Two arguments can be made to support this statement. First, the decay of OH or OD radicals is measured in the absence of reactant (HBr/DBr). Any reactivity under these conditions with Ar, N_2, OH(OD), or other radical species created in the flow due to the discharge is accounted for, and results in all or part of the nonzero intercept observed in the plot of k' vs [R] (Figure 3). Second, the large concentration of reactant added, HBr or DBr, allows for isolation of the process of interest, due to the concentration dependence of the decay of OH on R, through $d[OH]/dt = -k[OH][R]$. For the secondary processes to contribute significantly to the measured second order rate coefficients the concentration of the secondary species would have to be quite high, or the rate of the process be particularly faster than the rate of the primary process, or both; neither of which are likely. A number of the rates for secondary reactions (to our kinetic scheme) have been measured and are found to be either slow or rely on the formation of a reactive species such as Br_2 or H_2O_2. In particular measurements

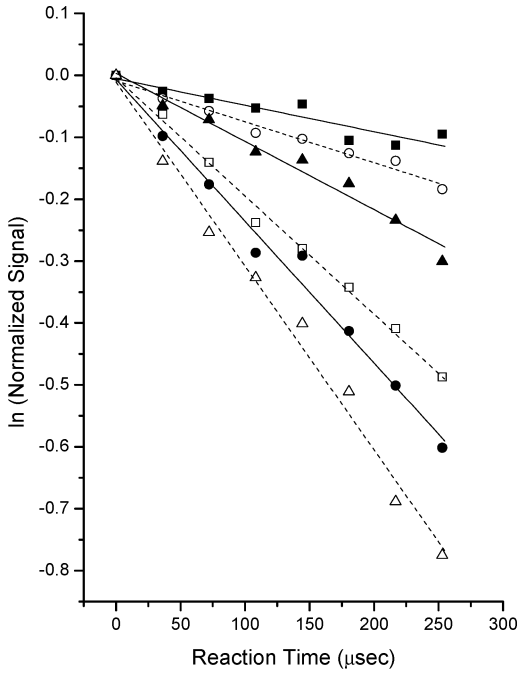

Figure 2. Pseudo-first order decays of the OH radical in the presence of HBr, for the reaction of OH + HBr at 53 K taken in the post ArM32e16 nozzle flow. % HBr in flow: ■, 0.00; ○, 0.04; ▲, 0.07; □, 0.14; ●, 0.17; △, 0.25.

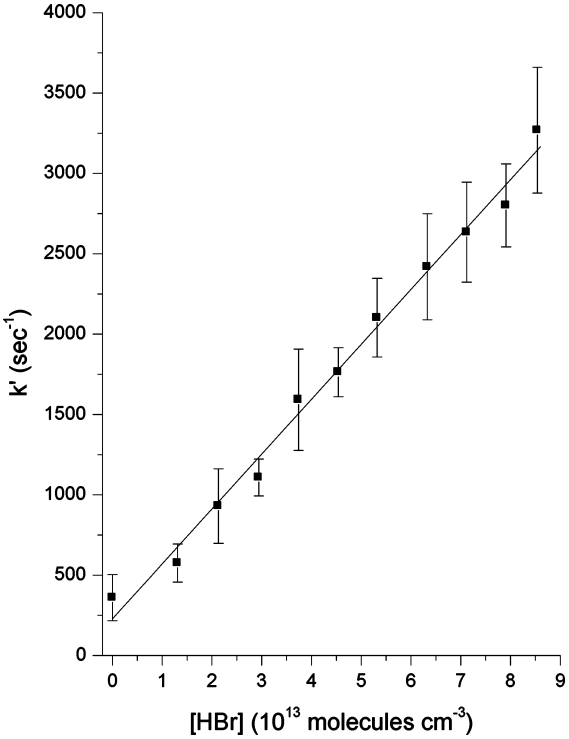

Figure 3. Graph of k' (s^{-1}) versus the concentration of HBr (10^{13} molecules/cm^3) for the OH + HBr reaction taken in the post ArM32e16 nozzle flow. The slope of this plot is used to extract the second order rate coefficient. Error bars on the experimental points are at the 2σ confidence limit and were obtained from linear least-squares fitting of the pseudo-first order decays of Figure 2.

TABLE 1: Calibrated Nozzle Flow Characteristics for the Nozzles Used in This Study

nozzle	mach no.	stagnation temp (K)	T_{flow} LIF (K)	T_{flow} impact (K)	flow density (10^{16} cm^{-3})
ArM32e16	3.5	263	53 ± 4	53 ± 3	3.2 ± 0.2
N2M32e16	3.2	273	83 ± 3	89 ± 5	1.7 ± 0.2
N2M33e16	2.5	300	135 ± 11	132 ± 6	4.5 ± 0.5

TABLE 2: Summary of the Rate Coefficients for the Reaction of OH + HBr and the H/D Isotopic Variants Measured in This Study

reaction	temp (K)	[R] (10^{13} cm^{-3})	k(10^{-11} cm^3 molecule^{-1} s^{-1})
OH + HBr	53	8.5	3.46 ± 0.15
OH + HBr	83	6.2	2.53 ± 0.21
OH + HBr	135	9.0	1.86 ± 0.21
OD + HBr	53	9.5	5.11 ± 0.29
OD + HBr	83	6.2	2.61 ± 0.16
OD + HBr	135	6.5	1.93 ± 0.25
OD + DBr	53	7.2	2.25 ± 0.14
OD + DBr	83	5.8	1.39 ± 0.12
OD + DBr	135	11.9	1.19 ± 0.13
OD + DBr	53	7.5	3.04 ± 0.16
OD + DBr	83	5.5	2.08 ± 0.17
OD + DBr	135	12.1	0.97 ± 0.15

of the isotope exchange channels

$$OH + DBr \rightarrow OD + HBr \quad (5)$$

$$OD + HBr \rightarrow OH + DBr \quad (6)$$

$$OH + D_2O \rightarrow OD + HOD \quad (7)$$

$$OD + H_2O \rightarrow OH + HOD \quad (8)$$

indicate that the upper limits for the rate coefficients are 3×10^{-14} and 1×10^{-13} cm^3/s at 298 K[23] and 3×10^{-13} and 5×10^{-13} cm^3/s at 141 K[24] for R5 and R6, respectively. An independent verification of these rates was not conducted at low temperatures in these studies. Similarly, the isotope exchange reactions R7 and R8 are known to be slow at room temperature with rates $<5 \times 10^{-17}$ and $(3.0 \pm 1.0) \times 10^{-16}$ cm^3/s.[30] These reactions are further highly unlikely to be occurring in the flow because the experiments were conducted in pure H_2O or D_2O precursor. In addition, the reactions of OH and OD radicals with Br_2[31] and OH with H_2O_2[32] have been studied in a temperature dependent fashion and shown to be reasonably fast at low temperature but again are highly unlikely to be influencing the kinetics of R1 through R4 due to the anticipated low concentration of the Br_2 and H_2O_2 species in the flow.

Results

The rates of reactions R1 through R4 were measured at three temperatures 53, 83, and 135 K under pseudo-first order conditions. Table 2 shows the temperature-dependent results. The errors reported in Table 2 are those at the 95% confidence limit. The value and error in each rate represents a weighted average and corresponding error in the mean with unequal uncertainties from a number of measurements.[33] Graphs of k vs T for R1 through R4 can be seen in Figure 4, parts a−d, respectively. Two fits to the functional form $k(T) = A(T/298)^{-n}$ are shown on each graph. They represent a fit to the low-temperature data set only, for this work, solid line, and the work of Jaramillo and Smith,[24] dashed line, extrapolated to higher temperatures so that the data could be compared to that of Bedjanian et al.[23] Figure 4a also depicts the data of Atkinson et al.[10] It can be seen for all cases, except for OD + HBr, good agreement between the measurements of this work and of Bedjanian et al. is realized. For the case of OD + HBr, Figure 4b, it appears that the steepness of the inverse temperature dependence in the region from 53 to 135 K, causes the rate calculated from the fit of the low temperature data only, to be underestimated in comparison to the measurement of Bedjanian et al. However, this underestimation can easily be overcome with a fit to both data sets but was not done here, as the goal was to illustrate the difference or similarity in the three data sets. Table 3 lists the best fit parameters obtained from fitting the data of this work to the power law form.

The data of Jaramillo and Smith[24] is seen to be markedly steep in all cases, and as a result, a reevaluation of the data was conducted. The errors reported in the original publication for the data measurements were the standard error and the final results (i.e., $k(T)$'s) represent the average of the measurements. In this study, the standard deviation was calculated as the square root of the sum of the squares of the individual standard errors divided by the number of measurements, as would be anticipated for a normal error probability function for a large number of measurements. However, in cases where the number of measurements is small, $N < 20$, it is desirable to use a statistical treatment of random errors to place a confidence limit on the mean, through use of the Student's t distribution which takes into account the joint probability that N observations fall within a certain range and the number of degrees of freedom in the system.[34] In this fashion, the raw data was re-plotted and a linear least squares regression analysis was used to extract the individual rates and errors in the rates at the 2σ (95%) confidence level. The weighted average and error in the average was then calculated in the same fashion as the numbers reported in the present study so that a direct comparison of the data could be made. Figure 5 shows the difference in the data before and after being treated in this way, for reactions R1 through R4. The revised data is used throughout the rest of this report. The change in the rate and the error associated with it is reflective of the quality of the data.

As mentioned in the Introduction, great interest in the temperature dependence of reaction R1 stems from its important role in the atmospheric chemistry of the Br atom. A new temperature-dependent fit of the global data set including this work has been done and can be seen in Figure 6. All of the data used for this graph are included in Table 4. A nonlinear least-squares fitting routine was used to fit the data to a power law and modified Arrhenius functional form, as shown in Figure 6. The fitting routine took into consideration the individual error bars associated with each data point and minimized the sum of the squares deviation. The shaded area represents the 95% confidence limit interval of the modified Arrhenius fit. The best fit parameters over the temperature range 23−360 K are found to be $k(T) = (1.06 \pm 0.02) \times 10^{-11}(T/298)^{(-0.90\pm0.11)}$ and $(0.96 \pm 0.02) \times 10^{-11}(T/298)^{(-0.90\pm0.03)} \exp^{((-2.88\pm 1.82\ K)/T)}$ cm^3/s.

The data of Table 2 from this work was used in conjunction with the revised data of Jaramillo and Smith and Bedjanian et al. to examine the kinetic isotope effects as a function of temperature over the region 53−360 K. The results for the primary kinetic isotope effect (PKIE) for common reactant OH and secondary kinetic isotope effect (SKIE) for common reactant HBr can be seen in Figure 7. Similarly, the results for the PKIE with common reactant OD and SKIE with common reactant DBr can be seen in Figure 8. The plots are presented in this fashion because they compare reactions that create similar products: in the case of Figure 7, HOD vs HOH, whereas for

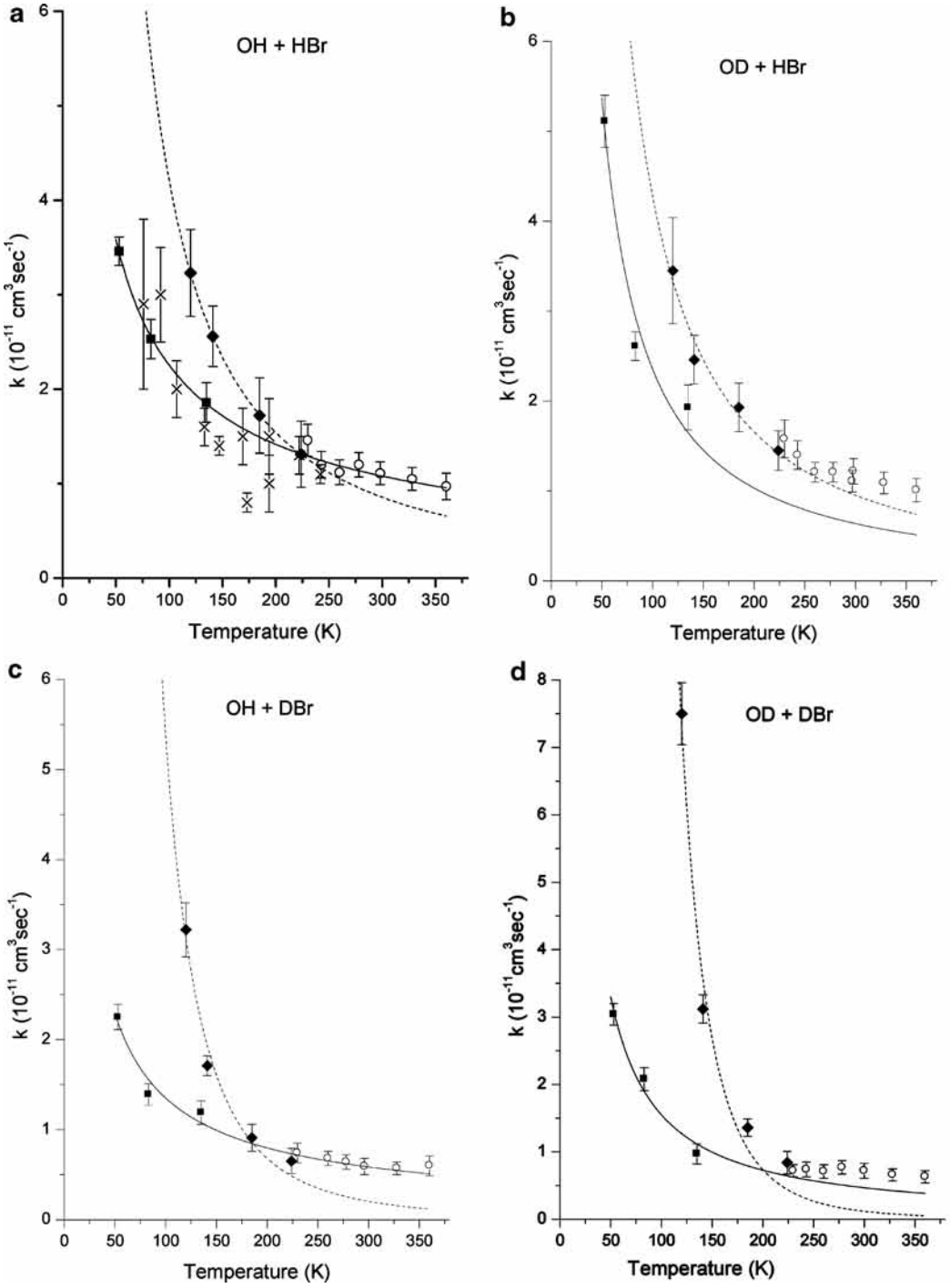

Figure 4. Temperature dependence of the rate coefficients for the reactions (a) OH + HBr, (b) OD + HBr, (c) OH + DBr, (d) OD + DBr: ■, this work; ×, Atkinson et al.;[10] ◆, Jaramillo and Smith;[24] ○, Bedjanian et al.[23] The fits displayed are to the functional form $k(T) = A(T/298)^{-n}$. Solid line is the fit to the data of this work, extrapolated to higher temperature for comparison to the data of Bedjanian et al. The dashed line is the fit to the Jaramillo and Smith data and extrapolated in the same manner.

TABLE 3: Best Fit Parameters to the $k(T) = A(T/298)^{-n}$ Power Law Functional Form for the OH + HBr and H/D Isotopic Variant Reactions

reaction	$A(10^{-12}$ cm^3 s$^{-1})$	$-n$
OH + HBr	10.84 ± 0.31	0.67 ± 0.02
OD + HBr	6.43 ± 2.60	1.19 ± 0.26
OH + DBr	5.89 ± 1.93	0.76 ± 0.22
OD + DBr	4.71 ± 1.56	1.09 ± 0.21

Figure 8, HOD vs DOD. Due to the scatter of the data, it was desirable to include a temperature-dependent fit to the data, to help guide the eye. The fits seen in Figures 7 and 8 were made by fitting the data of this work and that of Bedjanian et al. (Figure 4a−d) to the power law form, and using the appropriate ratio of the fits to predict the KIEs, in this manner reducing the statistical fluctuations in the data. Including the data of Jaramillo and Smith[24] caused the fits to shift off the data sets, and this data was not included for this reason. The fits to the KIE data show only a weak temperature dependence and yield values of $k_1/k_2 = (0.93 + 0.13, - 0.21)$, $k_1/k_3 = (1.75 + 0.09, - 0.16)$, $k_2/k_4 = (1.69 + 0.06, - 0.11)$, and $k_3/k_4 = (0.90 + 0.11, - 0.19)$, where the (+) and (−) indicate the range with respect to the average value. It can be seen that the fitting procedure provides reasonable agreement with the data except in the case of the 120 and 141 K PKIE (k_2/k_4) data of Jaramillo and Smith.

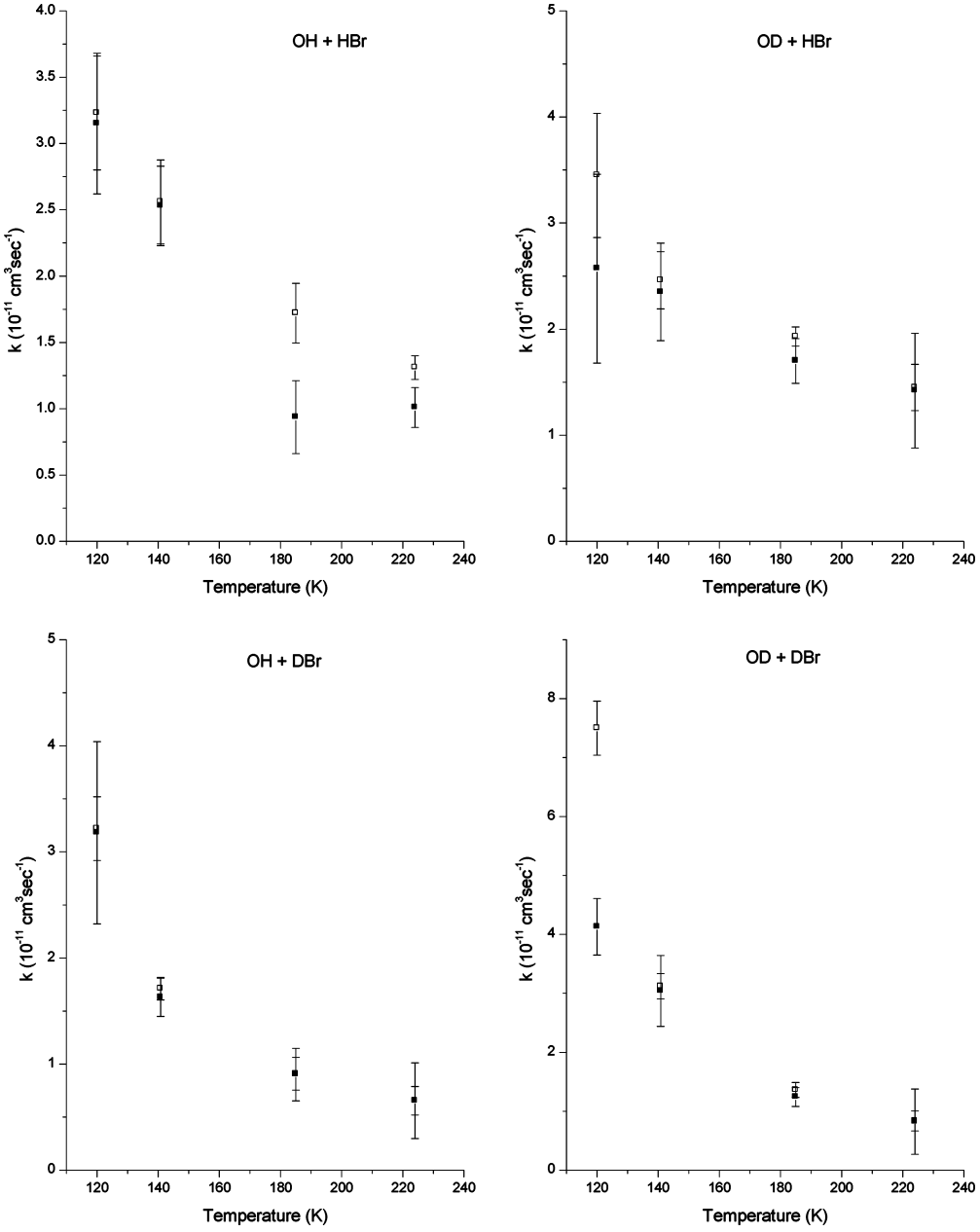

Figure 5. Comparison of the Jaramillo and Smith[24] data before and after revision for the OH + HBr and H/D isotopic variants reactions. Open symbols, original data; closed symbols, revised data.

Discussion

Reactions displaying inverse temperature dependence for a wide variety of systems are now widely known. These include the addition reactions of OH radicals with unsaturated hydrocarbons,[9,35,36] CN radical reactions,[37,38] various carbon atom reactions,[39−41] O(^{3}P) atom with unsaturated species,[42] and C_2H radical with a variety of species.[43−47] Although the manifestation of inverse temperature dependence is becoming commonplace, measurements of temperature dependent KIE ratios remain sparse. The inverse temperature dependence observed for these reactions has been attributed to the absence of a barrier along the reaction coordinate. At low temperature, fewer collisions are occurring on rotationally excited surfaces, causing the cross section for the process to increase. The rotating bond approximation applied by Clary et al.[25] has enjoyed success when applied to the heavy light heavy reactions of OH + HCl and HBr. In this work, a correlation was found between the reactant rotational states and the product bending states, leading to a rotationally enhanced cross section at low temperature with a $(B/T)^{1/2}$ temperature dependence that qualitatively described the experimental data. Unfortunately, calculations of the kinetic isotope effects for the OH + HBr system were not conducted. The current experimental findings are discussed in conjunction with the other systems that have been studied to date to create a framework within which the results can be understood. These include the temperature-dependent studies of the reactions of OH(D) + H(D)Cl, OH(D) + H(D)Br, and C_2H + $NH_3(D_3)$.

Battin-Leclerc et al. have studied the temperature-dependent KIE ratios for the OH + HCl and all isotopic variants using a pulsed laser photolysis-laser induced fluorescence flow reactor between 200 and 400 K.[48] They find a normal temperature-dependent PKIE (k_3/k_4 and k_1/k_2, using their nomenclature) that varies from approximately 2 to 6.5 over the temperature window of their experiment and indicate that H atom tunneling becomes significant at lower temperatures. They also conducted effective barrier calculations which indicate that the barrier decreases from

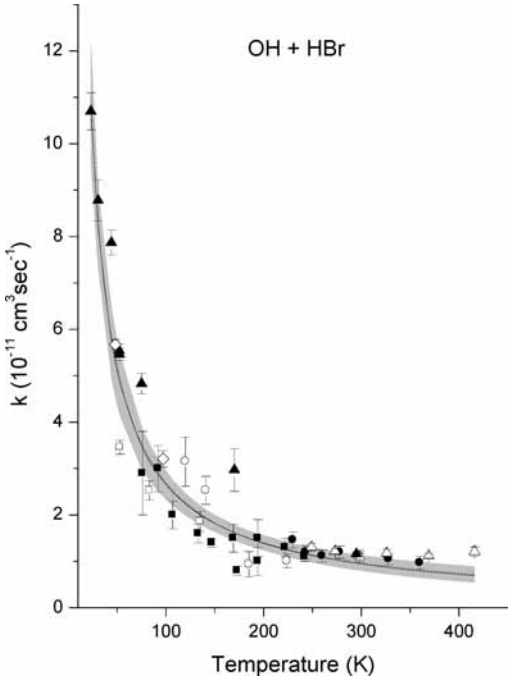

Figure 6. OH + HBr global fit to the temperature-dependent rate data over the 23−360 K window. □, This work; ■, Atkinson et al.;[10] ○, Jaramillo and Smith;[24] ●, Bedjanian et al.;[23] △, Ravishankara et al.;[8] ▲, Sims et al.;[9] ◇, Jaramillo et al.[12] The solid line is the fit to the power law functional form, and the dashed line is the fit to the modified Arrhenius form. Grey region is the 95% confidence interval of the fit.

12.22 to 9.71 kcal/mol in the series OH + HCl > OH + DCl > OD + HCl > OD + DCl, with the reduction in barrier height due to OD because of the zero-point energy difference and the lower frequency modes in the transition state. Although the primary KIE for OH + HCl gets quite high at low temperatures, qualitative agreement is seen between the portion of the PKIE not attributed to tunneling in the OH + HCl case and the PKIEs of this work for OH + HBr, $(k_1/k_3)_{Avg} = (k_2/k_4)_{Avg} = 1.64$ and the PKIE for OH + HBr of Bedjanian et al. $k_1/k_4 \approx k_3/k_5 \approx 1.7$. However, it should be noted that the OH + HCl system demonstrates a positive activation energy at all temperatures, whereas the OH + HBr reaction shows no indication of a positive barrier. It is not clear how to directly compare the kinetic isotope effects for reactions occurring over seemingly quite different potential energy surfaces.

The SKIE's for OH + HCl observed in Battin-Leclerc et al.[48] are inverse in nature and vary from approximately 0.83 to 0.95, with the k_1/k_3 (common HCl) ratio showing stronger temperature dependence than that of k_2/k_4 (common DCl). Again, these ratios are in accord with those observed in this study, $(k_1/k_2)_{Avg} = 0.87$ and $(k_3/k_4)_{Avg} = 0.88$ for OH + HBr. Similarly, Bedjanian et al. receive SKIE ratios of $k_1/k_3 \approx k_4/k_5 \approx 1$ for OH + HBr.[23] The results of the three studies seem to indicate that the secondary kinetic isotope effect is most sensitive to the transition state for these two reactions, even though both occur over different potential energy surfaces. The creation of the lower frequency vibrational modes due to the spectator nature of the OD bond and its correlation to water product states appears to have a greater influence on the dynamics than it does from the changes in number of states in the reactant manifold due to zero-point effects.

More recently Nizamov and Leone have investigated the reactions of C_2H with NH_3 and ND_3 in a pulsed Laval nozzle apparatus, at three temperatures of 104 ± 5, 165 ± 15, and 296 ± 2 K.[44] They find that in accord with theoretical predictions that the reaction proceeds via the exothermic ($\Delta H^\circ_{298K} = -121$ kJ/mol) hydrogen abstraction mechanism without a barrier, demonstrated by the strong negative temperature dependence observed. In addition, and relevant to the OH + HBr system, they observe a rather large PKIE of (2.0 ± 0.2) independent of temperature over the range investigated. Although they acknowledge that precise knowledge of the observed KIE cannot be judged without accurate calculations, the authors suggest the origin of the large KIE could be contributions from tunneling. Alternatively, from a statistical standpoint, the KIE could be due to an increase in the reactant rotational density of states upon deuteration, without significant effects on the activated complex, leading to a temperature independent kinetic isotope effect. Further, they argue that explanation of the kinetic isotope effect based solely on changes in zero-point energies is inconsistent with the temperature independence of the KIE. This is due to the $\exp(-\Delta E_0^{\ddagger}/kT)$ factor that is obtained when the k_H/k_D ratio is derived from classical transition state theory, but they also mention that application of classical transition state theory may be too simplistic for reaction systems occurring over potential energy surfaces without a barrier. It is also interesting that the temperature dependence observed for the $NH_3 + C_2H$ system $T^{(-0.90\pm0.15)}$ is in accord with the temperature dependence observed in this study for OH + HBr and all of the isotopic variants, within the errors quoted. It seems that these two

TABLE 4: OH + HBr Rate Data Used to Obtain the Temperature Dependent Global Fit in Figure 6

investigator	temp (K)	rate (10^{-11}cm^3/s)	error
Jaramillo and Smith[24]	120	3.15	0.53
	140.8	2.53	0.3
	185	0.936	0.274
	224	1.01	0.15
Bedjanian et al.[23]	230	1.46	0.17
	243	1.2	0.14
	260	1.12	0.13
	278	1.2	0.13
	298	1.11	0.12
	328	1.05	0.12
	360	0.97	0.14
Ravishankara et al.[8]	249	1.31	0.08
	273	1.22	0.05
	298	1.11	0.07
	326	1.18	0.08
	369	1.12	0.05
	416	1.21	0.1
Sims et al.[9]	23	10.7	0.4
	30.5	8.78	0.44
	44	7.87	0.27
	52.1	5.54	0.15
	52.3	5.46	0.13
	75	4.83	0.22
	170	2.97	0.46
	295	1.16	0.04
Jaramillo et al.[12]	48	5.67	0.11
	97	3.21	0.18
Atkinson et al.[10]	242	1.1	0.1
	222	1.3	0.2
	194	1	0.3
	194	1.5	0.4
	173	0.8	0.1
	169	1.5	0.3
	147	1.4	0.1
	133	1.6	0.2
	107	2	0.3
	92	3	0.5
	76	2.9	0.9
This work	53	3.46	0.15
	83	2.53	0.21
	135	1.86	0.21

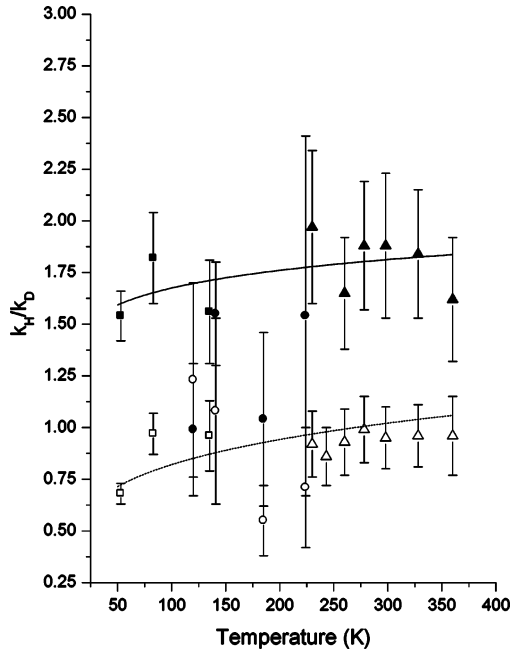

Figure 7. Primary and secondary kinetic isotope effects (k_H/k_D) plotted versus temperature for the OH + HBr and H/D isotopic variants reactions. k_1 and k_3 share the common reactant OH, whereas k_1 and k_2 share the common reactant HBr. Closed symbols are for the primary kinetic isotope effect (k_1/k_3): ■, this work; ●, Jaramillo and Smith;[24] ▲, Bedjanian et al.[23] Open symbols are for the secondary kinetic isotope effect (k_1/k_2): □, this work; ○, Jaramillo and Smith;[24] △, Bedjanian et al.[23]

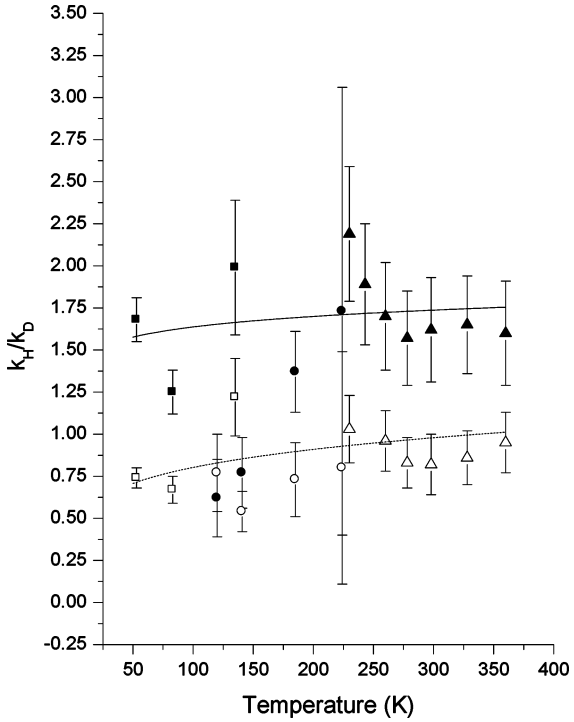

Figure 8. Primary and secondary kinetic isotope effects (k_H/k_D) plotted versus temperature for the OH + HBr and H/D isotopic variants reactions. k_2 and k_4 share the common reactant OD, whereas k_3 and k_4 share the common reactant DBr. Closed symbols are for the primary kinetic isotope effect (k_2/k_4): ■, this work; ●, Jaramillo and Smith;[24] ▲, Bedjanian et al.[23] Open symbols are for the secondary kinetic isotope effect (k_3/k_4): □, this work; ○, Jaramillo and Smith;[24] △, Bedjanian et al.[23]

abstraction reactions, although differing in the number of degrees of freedom, share similar characteristics due to the large exothermicity involved and the lack of a barrier.

A number of theoretical efforts have also been conducted aimed at understanding the negative temperature dependence, the vibrational energy distribution imparted to the exiting H_2O molecule, and the kinetic isotope effects observed for OH + HBr and isotopic variants. The observed temperature dependence of reaction R1 is best fit by a $T^{-0.90}$ functional form, and this dependence is consistent with that calculated using quantum scattering calculations with the rotating bond approximation using a LEPS surface.[25] Nizamov et al.[26] performed quasiclassical trajectory calculations (QCT) to explore the dynamics of reactions R1 and R2 using the Clary potential and a modified form adjusted to match the fraction of H_2O vibrational energy dispersal experimentally measured by Butkovskaya and Setser.[27] They also employed variational transition state theory to obtain rate constants that could be compared to the QCT and experimental values. They find the transition state to lie at a classical energy of ~ -1.75 kcal/mol with respect to reactants, and with harmonic zero-point adjustment, the barrier shifts to -0.12, $+0.06$, and -0.23 kcal/mol, for the Clary OH + HBr PES, the modified OH + HBr PES, and the modified OD + HBr PES, respectively. Due to the fact that the zero-point adjusted barrier was lower for OD + HBr by 0.29 kcal/mol than for OH + HBr, an inverse SKIE (k_1/k_2) was predicted and attributed to the difference in DOH vs HOH bending frequencies in the transition state. At 300 K, the VTST rates calculated on the modified potential predict a SKIE of 0.76. Although a bit low, the SKIE value predicted by the VTST calculation is in qualitative agreement with the measurements of this work and Bedjanian et al.[23]

An inverse PKIE (k_1/k_3) of 0.72 is also calculated in the Nizamov et al. study[26] which is similar in magnitude to the SKIE calculated at 300 K using the modified potential. Again, the PKIE arises due to a lowering of the zero-point energy adjusted barrier for OH + DBr relative to OH + HBr. However, the authors note that large k_H/k_D values are difficult to explain by any transition state model, when the transition state is located early in the entrance channel, because the HBr and DBr frequencies are similar in the reactants and transition state. The lack of agreement between the PKIE experimentally measured at 300 K ($k_H/k_D \approx 1.7$)[23] and calculated using the semiempirical surface is therefore not terribly surprising.

Direct ab initio dynamics calculations of the reaction rates for the OH + HBr reaction have also been conducted.[28] The goal of using this approach was to obtain dynamical information on an accurate potential energy surface obtained from accurate ab initio electronic structure calculations. The study finds that on the reactant side of the potential energy surface there is a hydrogen bonded complex (HBC) lower in energy than reactants by -1.71 kcal/mol, which looks similar in geometry to the transition states calculated in the quantum scattering[25] and QCT calculations.[26] The reaction is found to pass through a reactant-like transition state with an energy slightly higher in energy than that of the reactants (0.89 kcal/mol) in going from the HBC to products. Further, the rates of reaction are calculated using improved canonical variational transition state theory (ICVT) and with a small curvature tunneling correction (ICVT/SCT). Qualitative agreement is found between the rates calculated and those found experimentally, but the ratio of the rate coefficients calculated ([ICVT/SCT]/ICVT) is found to be dependent on temperature, with the ICVT/SCT gaining importance as the temperature is reduced, indicating the importance of tunneling to the reaction at low temperatures. If this is indeed true, one might understand the tunneling contribution to the atom transfer as being responsible for the normal PKIE observed experimen-

tally. The finding by Liu et al.[28] that the reaction proceeds via an "early" transition state which is reactant-like in nature also indicates that the reaction is more sensitive to the reactant energies than to changes in the transition state frequencies upon deuteration.

It seems reasonable to suggest that the KIE ratios are constant over the temperature range explored in this study and that of Bedjanian et al.[23] Locating the origin of the effect, however, is a bit more difficult. From a transition state theory perspective, for a reaction occurring over a potential energy surface with a barrier, the KIE ratio arises due to differences in zero-point energies and the rotational, vibrational, and translational partition functions according to eq 5

$$\frac{k_H}{k_D} = \left(\frac{Q^{Trans}_{HOHBr}}{Q^{Trans}_{DOHBr}}\frac{Q^{Trans}_{OD}}{Q^{Trans}_{OH}}\right)\left(\frac{Q^{Vib}_{HOHBr}}{Q^{Vib}_{DOHBr}}\frac{Q^{Vib}_{OD}}{Q^{Vib}_{OH}}\right)\left(\frac{Q^{Rot}_{HOHBr}}{Q^{Rot}_{DOHBr}}\frac{Q^{Rot}_{OD}}{Q^{Rot}_{OH}}\right)\left(\frac{Q^{Inter}_{HOHBr}}{Q^{Inter}_{DOHBr}}\right)\exp^{([E_{HOHBr}-E_{DOHBr}]/k_bT)} \quad (5)$$

where Q_{Trans}, Q_{Vib}, and Q_{Rot} represent the translational, vibrational, and rotational partition functions, respectively. Q_{Inter} represents the partition function associated with motion along the reaction coordinate, the exponential term is the difference in activation energy at the transition state, k_b is Boltzmann's constant, with the reactant partition function indicated by the subscript OH(D) and the transition state partition function by the subscript H(D)OHBr. Equation 5 represents the situation for the SKIE. The expression for the PKIE is similar, with HBr and DBr substituted into the reactants and transition state. Deuteration of either of the reactants leads to changes in the reactant partition functions of Q_{Vib}, Q_{Rot}, and Q_{Trans}. These can be estimated, but it is the transition state partition functions and energetics that make assessment of the origin of the observed KIEs difficult, due to the necessity of an accurate potential energy surface. Even with an assumed transition state geometry, state sums and densities have been difficult to assess due to anharmonic effects, as pointed out by Nizamov et al.[26] Further, the difference in zero-point energy of the transition state for the deuterated vs nondeuterated case should introduce a temperature dependence to the KIE, although it is not clear at this time to what extent. One might argue that the rotational dependence of the cross section offsets the temperature dependence predicted by transition state theory, or that the exponential term of eq 5 is not appropriate for reactions occurring without an apparent barrier, and these points certainly warrant further investigation.

As previously mentioned, Nizamov et al. attribute the PKIE (k_1/k_3) and SKIE (k_1/k_2) to a lowering of the zero-point adjusted barriers for the deuterated reactions. At 300 K, the inverse SKIE observed experimentally is reasonably well reproduced by theory and is understood to occur due to the difference in the DOH vs HOH bending frequency in the transition state. A rigorous understanding of the origin of the PKIE, however, is not. A temperature-dependent expression for the inverse PKIE of Nizamov et al. is provided in that study, which indicates an increased reaction efficiency of k_D vs k_H as the temperature is lowered. Since neither the absolute value of the PKIE nor the temperature dependence of the PKIE calculated appear to be observed experimentally, it is unclear whether it is a limitation in transition state theory to accurately predict KIEs, as suggested by Nizamov et al., or whether it is another offsetting factor, such as tunneling, as suggested by the calculations of Liu et al.,[28] that leads to the discrepancy.

Questions naturally arise regarding the difference in the data measured using the pulsed supersonic Laval nozzle flow reactor in Tucson. The scatter in the data of Jaramillo and Smith[24] is thought to reflect statistical or systematic errors in the data obtained in those studies. Oftentimes rates were extracted from k' vs [R] plots containing four or five data points with considerable deviation from linearity. Therefore, the error bars most likely under represent the true error associated with the measurements. Part of the scatter could have been introduced by the method by which the HBr and DBr concentrations were calculated. These concentrations were calculated from a measurement of the absorption cross section at 220 nm (near the threshold), so that the absorbance measured in the reactant delivery line, in conjunction with the flow rate and line pressure, could be converted into an absolute concentration in the flow. It is difficult to determine whether these measurements suffered from systematic errors due to baseline drift in the absorption spectrometer or from adsorption of HBr and DBr molecules onto window surfaces. Other sources of error such as improper nozzle calibration leading to un-equilibrated flow and nonuniform flow are also candidates. In the present study, care was taken to ensure that the flow was continually monitored to ensure reliable flow conditions, and the HBr and DBr concentrations were calculated solely from the gas flow rate, so that errors associated with the absorption measurement could be minimized.

Conclusion

The rates of reaction for the OH + HBr and H/D isotopic variants have been measured between 53 and 135 K using a pulsed supersonic Laval nozzle flow reactor. For the OH + HBr system, the new low-temperature results are found to be in accord with the measurements of Atkinson et al.,[10] but systematically lower than the studies of Jaramillo and Smith,[24] Jaramillo et al.,[12] and Sims et al.,[11] however these data does not alter our interpretation of the temperature dependence of reaction R1. It most likely highlights the difficulty of working with HBr at low temperatures.

The KIE's were also investigated and found to be independent of temperature between 53 and 135 K. These results seem to be in accord with the study of Bedjanian et al.[23] However, a theoretical study capable of accurately treating the nature of the electronic surface and the zero-point energy adjusted barriers would surely lend insight into the dynamics leading to the kinetic isotope effects measured for reactions R1 through R4.

Acknowledgment. The authors gratefully acknowledge financial support of this work by the National Science Foundation through Grant No. CHE-9984613.

References and Notes

(1) Ravishankara, A. R.; Wine, P. H.; Langford, A. O. *Chem. Phys. Lett.* **1979**, *63*, 479.

(2) Takacs, G. A.; Glass, G. P. *J. Phys. Chem.* **1973**, *77*, 1060.

(3) Smith, I. W. M.; Zellner, R. *J. Chem. Soc., Faraday Trans.* **1974**, *8*, 1045.

(4) Wilson, W. E. J.; Donovan, J. T.; Fristrom, R. M. 12th Symposium on Combustion, 1969.

(5) Cannon, B. D.; Robertshaw, J. S.; Smith, I. W. M.; Williams, M. D. *Chem. Phys. Lett.* **1984**, *105*, 380.

(6) Jourdain, J. L.; Lebras, G.; Combourieu, J. *Chem. Phys. Lett.* **1981**, *78*, 483.

(7) Husain, D.; Plane, J. M. C.; Slater, N. K. H. *J. Chem. Soc., Faraday Trans.* **1981**, *77*, 1949.

(8) Ravishankara, A. R.; Wine, P. H.; Wells, J. R. *J. Chem. Phys.* **1985**, *83*, 447.

(9) Sims, I. R.; Smith, I. W. M.; Bocherel, P.; Defrance, A.; Travers, D.; Rowe, B. R. *J. Chem. Soc., Faraday Trans.* **1994**, *90*, 1473.

(10) Atkinson, D. B.; Jaramillo, V. I.; Smith, M. A. *J. Phys. Chem. A* **1997**, *101*, 3356.
(11) Sims, I. R.; Smith, I. W. M.; Clary, D. C.; Bocherel, P.; Rowe, B. R. *J. Chem. Phys.* **1994**, *101*, 1748.
(12) Jaramillo, V. I.; Gougeon, S.; Le Picard, S. D.; Canosa, A.; Smith, M. A.; Rowe, B. R. *Int. J. Chem. Kinet.* **2002**, *34*, 339.
(13) Atkinson, R.; Baulch, D. L.; Cox, R. A.; Hampson, R. F.; Kerr, J. A.; Rossi, M. J.; Troe, J. *J. Phys. Chem. Ref. Data* **1997**, *26*, 521.
(14) DeMore, W. B.; Sander, S. P.; Golden, D. M.; Hampson, R. F.; Kurylo, M. J.; Howard, C. J.; Ravishankara, A. R.; Kolb, C. E.; Molina, M. J. *Chemical Kinetics and Photochemical Data For Use in Stratospheric Modeling*; NASA, JPL, California Institute of Technology: CA, 1997.
(15) Aikawa, Y.; Herbst, E. *Astrophys. J.* **1999**, *526*, 314.
(16) Gerlich, D.; Schlemmer, S. *Planet. Space Sci.* **2002**, *50*, 1287.
(17) Roberts, H.; Herbst, E.; Millar, T. J. *Mon. Not. R. Astron. Soc.* **2002**, *336*, 283.
(18) Millar, T. J. *Planet. Space Sci.* **2002**, *50*, 1189.
(19) Croswell, K.; Dalgarno, A. *Astrophys. J.* **1985**, *289*, 618.
(20) Roberts, H.; Millar, T. J. *Astron. Astrophys.* **2000**, *361*, 388.
(21) Lunine, J. I.; Lorenz, R. D.; Hartmann, W. K. *Planet. Space Sci.* **1998**, *46*, 1099.
(22) Smith, I. W. M.; Rowe, B. R. *Acc. Chem. Res.* **2000**, *33*, 261.
(23) Bedjanian, Y.; Riffault, V.; Le Bras, G.; Poulet, G. *J. Photochem. Photobiol. A: Chem.* **1999**, *128*, 15.
(24) Jaramillo, V. I.; Smith, M. A. *J. Phys. Chem. A* **2001**, *105*, 5854.
(25) Clary, D. C.; Nyman, G.; Hernandez, R. *J. Chem. Phys.* **1994**, *101*, 3704.
(26) Nizamov, B.; Setser, D. W.; Wang, H.; Peslherbe, G. H.; Hase, W. L. *J. Chem. Phys.* **1996**, *105*, 9897.
(27) Butkovskaya, N. I.; Setser, D. W. *J. Phys. Chem.* **1996**, *100*, 4853.
(28) Liu, J. Y.; Li, Z. S.; Dai, Z. W.; Huang, X. R.; Sun, C. C. *J. Phys. Chem. A* **2001**, *105*, 7707.
(29) Mullen, C.; Smith, M. A. *J. Phys. Chem. A* **2005**, *109*, 1391.
(30) Dubey, M. K.; Mohrschladt, R.; Donahue, N. M.; Anderson, J. G. *J. Phys. Chem. A* **1997**, *101*, 1494.
(31) Bedjanian, Y.; Le Bras, G.; Poulet, G. *Int. J. Chem. Kinet.* **1999**, *31*, 698.
(32) Vakhtin, A. B.; McCabe, D. C.; Ravishankara, A. R.; Leone, S. R. *J. Phys. Chem. A* **2003**, *107*, 10642.
(33) Bevington, P. R. *Data Reduction and Error Analysis for the Physical Sciences*; McGraw-Hill Book Company: New York, 1969.
(34) Shoemaker, D. P.; Garland, C. W.; Nibler, J. W. *Experments in Physical Chemistry*, 6th ed.; The McGraw-Hill Companies, Inc.: New York, 1996.
(35) Vakhtin, A. B.; Murphy, J. E.; Leone, S. R. *J. Phys. Chem. A* **2003**, *107*, 10055.
(36) Vakhtin, A. B.; Lee, S.; Heard, D. E.; Smith, I. W. M.; Leone, S. R. *J. Phys. Chem. A* **2001**, *105*, 7889.
(37) Sims, I. R.; Queffelec, J.-L.; Travers, D.; Rowe, B. R.; Herbert, L. B.; Karthaeuser, J.; Smith, I. W. M. *Chem. Phys. Lett.* **1993**, *211*, 461.
(38) Sims, I. R.; Queffelec, J. L.; Defrance, A.; Rebrion-Rowe, C.; Travers, D.; Rowe, B. R.; Smith, I. W. M. *J. Chem. Phys.* **1992**, *97*, 8798.
(39) Chastaing, D.; Le Picard, S. D.; Sims, I. R. *J. Chem. Phys.* **2000**, *112*, 8466.
(40) Clary, D. C.; Buonomo, E.; Sims, I. R.; Smith, I. W. M.; Geppert, W. D.; Naulin, C.; Costes, M.; Cartechini, L.; Casavecchia, P. *J. Phys. Chem. A* **2002**, *106*, 5541.
(41) Chastaing, D.; James, P. L.; Sims, I. R.; Smith, I. W. M. *Phys. Chem. Chem. Phys.* **1999**, *1*, 2247.
(42) Huie, R. E.; Herron, J. T. *Prog. React. Kinet.* **1975**, *8*, 1.
(43) Nizamov, B.; Leone, S. R. *J. Phys. Chem. A* **2004**, *108*, 1746.
(44) Nizamov, B.; Leone, S. R. *J. Phys. Chem. A* **2004**, *108*, 3766.
(45) Murphy, J. E.; Vakhtin, A. B.; Leone, S. R. *Icarus* **2003**, *163*, 175.
(46) Vakhtin, A. B.; Heard, D. E.; Smith, I. W. M.; Leone, S. R. *Chem. Phys. Lett.* **2001**, *344*, 317.
(47) Chastaing, D.; James, P. L.; Sims, I. R.; Smith, I. W. M. *Faraday Discuss.* **1998**, *109*, 165.
(48) Battin-Leclerc, F.; Kim, I. K.; Talukdar, R. K.; Portmann, R. W.; Ravishankara, A. R. *J. Phys. Chem. A* **1999**, *103*, 3237.